IEEE Access
Multidisciplinary | Rapid Review | Open Access Journal

Received November 21, 2019, accepted November 28, 2019, date of publication December 2, 2019,
date of current version December 12, 2019.

Digital Object Identifier 10.1109/ACCESS.2019.2957032

Separation Behaviour Difference Between Gelatin and Porcine Liver Under High-Speed Waterjet Impact

CHAO CAO[1,2], JIYUN ZHAO[1,2], GUILIN LI[3], HAIGANG DING[1,2], XIN JIN[3], AND LIANGCHEN SONG[1,2]

[1]School of Mechatronic Engineering, China University of Mining and Technology, Xuzhou 221116, China
[2]Jiangsu Key Laboratory of Mine Mechanical and Electrical Equipment, China University of Mining and Technology, Xuzhou 221116, China
[3]Xuzhou Maternal and Child Health Care Hospital, Xuzhou Medical University, Xuzhou 221000, China

Corresponding authors: Jiyun Zhao (z874367650@163.com) and Guilin Li (568707641@qq.com)

This work was supported in part by the Priority Academic Program Development of Jiangsu Higher Education Institutions (PAPD), and in part by the Research Fund for Science and Technology Innovation of Xuzhou under Grant KC16SY155.

ABSTRACT Different from the rigid separation of biological tissue by scalpel, medical waterjet technology utilizes the impact kinetic energy of high-speed waterjet to instantly destroy the surface of biological tissue to achieve better clinical separation effect. Since the gelatin samples are transparent biomaterials, they were taken as the only substitute for soft tissue in experimental studies and observation in the current studies of medical waterjet separation technology, but the mechanical behavioural difference between the two has not been reported. To verify the adaptability of gelatin as a substitute of soft tissue under the impact of high-speed waterjet. Firstly, the dynamic process of impact was described through the energy balance equation. Then, based on the principle of altering a single variable, the difference of damage depth between 8 wt. %, 10 wt. %, and 12 wt. % gelatin samples and porcine liver tissue under various impact pressure, impact distance, and waterjet speed of motion (as opposed to flow velocity) was compared. The results show that the gelatin sample replicates the damage behaviour of porcine liver samples under the specific waterjet impact conditions, and the direction of the waterjet hydraulic power optimisation of the two materials is also consistent: however, due to the different sampling sites and anisotropy of porcine liver samples, the mechanical response of soft tissue under high-speed waterjet impact cannot be fully expressed by gelatin samples. The experimental results can provide support for the further study of medical waterjet separation technology.

INDEX TERMS High-speed impact, medical waterjet, separation behavior, surgical instruments, tissue engineering.

I. INTRODUCTION

Medical waterjet separation technology uses a very fine high-speed waterjet to impact the biological tissue, so that the biological tissue is deformed in an instant to achieve the separation effect: the transient impact of the waterjet prevents damage to biological tissue that does not need to be separated and maintains a clear field of vision within the surgical area. Compared to using a scalpel, medical waterjet separation technology provides significant advantages such as a smooth incision and less bleeding during surgery. Clinical practice shows that there are differences in the separation pressure of different tissues. It is indicated that studying the medical adaptability of high-speed waterjet to improve the protection afforded to specific tissues is an important development in medical waterjet separation technology in the future, therefore, analysis of medical waterjet separation mechanism and adaptive regulation strategy is important for development of the precise application of medical waterjet technology to improve post-surgery outcomes. Among them, experimental observation is an essential part of the soft tissue separation process. The flow of water during medical waterjet separation creates obstacles to the measurement of the force between the waterjet and the soft tissue, so behavioural observation

The associate editor coordinating the review of this manuscript and approving it for publication was György Eigner.

of soft tissue under high-speed waterjet impact becomes critical.

Due to the availability of materials, ease of preparation, and ethical significance, gelatin is increasingly replacing natural biological tissues for research applications [1], [2] in medical engineering, including forensic and military wound profiling, projectile damage simulation [3], [4], as medical phantom materials in imaging [5], [6], tissue regeneration materials [7], [8], and tissue substitutes in surgical simulations [9]; however, previous research has focused on the damage behaviour of gelatin under high-speed rigid impact. The impact velocity of a high-speed waterjet exceeds that under rigid separation, and the functional characteristics thereof are unclear. The adaptability of gelatin as a substitute under the impact of a high-speed waterjet needs to be verified.

In recent years, since the gelatin samples are transparent biomaterials, gelatin has been used in the research of medical waterjet separation technology to replace biological soft tissue for experiments and dynamic observations. Bahls *et al.* planned the optimal path for surgical robot operations based on 10 wt.% gelatin damage depth at a speed of 5 mm/s [10]; Seto *et al.* observed crack growth trends in 20 wt.% gelatin under high-speed waterjet impact, and compared the effects of different outlet diameters and piezoelectric drive frequencies on gelatin destruction efficiency [11]. Due to the differences in the material properties of different concentrations of gelatin samples, to clarify the behaviour difference between bio-soft tissue and gelatin under high-speed water-jet impact, and validate the feasibility of gelatin as an alternative material, will help to improve waterjet separation technology. To solve the above problems, this study starts with water hammer theory and energy analysis under a high-speed waterjet impinging on soft tissue, indicating that the differences in fluid dynamics, mode of operation, and target will affect the separation effect. Furthermore, to match clinical operating conditions, the impact distance, waterjet travel, and waterjet impact pressure were set as variables.

II. WATERJET IMPACT

A. WATER HAMMER

For the waterjet impact on a solid material, the instantaneous impact of the waterjet on a solid surface includes water hammer pressure and stagnation pressure [12], [13].

As shown in Figure 1, the impact of a free waterjet on soft tissue is divided into the following stages: at $t = 0$, the high-speed waterjet tip contacts the soft tissue surface; from t to t_1, the shock wave is formed at the contact point and propagates in the water and soft tissue at different speeds, the pressurized water medium is densely populated in the waterjet tip, and the soft tissue is elastically deformed; from t_1 to t_2, the waterjet stream continues to impact the soft tissue surface to form a new shock wave, because the velocity of the shock wave is much higher than the velocity of the waterjet, the water hammer pressure generated by the impact at its centre is disturbed by the shock wave until the waterjet tip is in complete

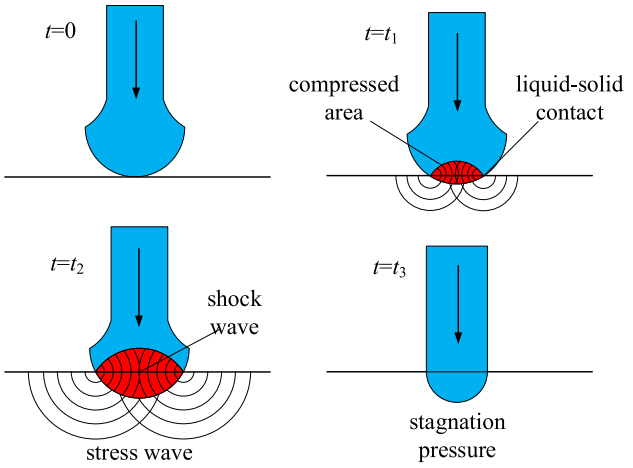

FIGURE 1. Waterjet hammer impact on soft tissue.

contact with soft tissue; at $t > t_3$ the waterjet impact will form a stable Bernoulli stagnation pressure from the dynamic pressure of the waterjet, and the waterjet centre-pressure is significantly reduced. Experimental studies have shown that the water hammer pressure has a short duration of action, on the order of nanoseconds [14], [15].

The following simplifications and assumptions are made for the above physical processes: (1) a uniform cylinder with the waterjet centred symmetrically; (2) when the waterjet contacts the soft tissue, the radial change at the waterjet tip is centre-symmetric; (3) the effects of gravity and friction are not considered.

It is assumed that at $t = 0$, the waterjet strikes the soft tissue surface with v_n. After a short period of time Δt, the surface of the soft tissue is deformed, and the absolute velocity of the waterjet and soft tissue on both sides of the contact surface becomes $v_n + v_w$ and v_t, respectively, and the absolute speeds of the two are equal at the contact point, namely:

$$v_n + v_w = v_t \tag{1}$$

Since momentum is conserved before and after impact:

$$F_w \cdot \Delta t = -\rho_w A \Delta t c_w v_w \tag{2}$$

$$F_t \cdot \Delta t = -\rho_t A \Delta t c_t v_t \tag{3}$$

where, F_w and F_t are respectively the force exerted by water and soft tissue on the contact surface. ρ_w and ρ_t represent density of water and soft tissue respectively; A is the area of the contact surface between the two; c_w and c_t are respectively the propagation velocity of the shock wave in water and soft tissue.

The force exerted on the fluid and soft tissue at the contact point is the reciprocal force, namely $F_w = F_t$, then

$$-\rho_w c_w v_w = \rho_t c_t v_t \tag{4}$$

Combining equations (1) and (4) into (2) and (3) gives:

$$F_t = \frac{\rho_w c_w \rho_t c_t A v_n}{\rho_w c_w + \rho_t c_t} \tag{5}$$

Therefore, the water hammer pressure P_h is given by

$$P_h = \frac{F_t}{A} = \frac{\rho_w c_w \rho_t c_t v_n}{\rho_w c_w + \rho_t c_t} \tag{6}$$

When the shock wave propagates to the waterjet boundary, the water hammer pressure vanishes, and this time of action can be calculated by using the distance and velocity. After the water hammer pressure vanishes and the waterjet force is stabilised, the stagnation pressure P_s at the centre of the waterjet is its axial dynamic pressure, that is,

$$P_s = \frac{\rho_w v_n^2}{2} \tag{7}$$

B. ENERGY BALANCE

The waterjet continuously strikes the surface of the soft tissue, and the surface of the soft tissue is deformed until soft tissue destruction begins. The soft tissue begins to break and the cracks therein continue to grow under the action of the fluid. According to the energy balance relationship [16], the kinetic energy and potential energy of the fluid are converted into the energy required for the formation of soft tissue cracks, stored elastic strain energy, and that stored under inelastic strain [17].

$$\Delta E = W_f + W_v + W_e \tag{8}$$

where ΔE represents fluid kinetic energy and potential energy changes, W_f is the work done by the waterjet striking the soft tissue to form a slit, W_v is the inelastic strain energy dissipated during the impacting process due to viscoelastic deformation, stress relaxation, creeping and micro-cracking, W_e is the elastic strain energy stored in the deformed zone.

Within unit time dt, the new waterjet carries kinetic and gravitational potential energy to impact soft tissue, namely

$$\Delta E = 1/2 dm v_n^2 + dmgv_n dt \tag{9}$$

where dm is the increase in fluid mass per unit time dt, v_n refers to the velocity of the waterjet, and g is the acceleration due to gravity, thus:

$$dm = \rho_w \pi R^2 v_n dt \tag{10}$$

$$\Delta E = \pi \rho_w R^2 \left(\frac{1}{2} v_n^3 dt + g v_n^2 d^2 t \right) \tag{11}$$

where ρ_w is the density of the water and R is the radius of the waterjet stream. Furthermore, in unit time dt, Equation (8) can be written as

$$\Delta E = JdA + d\Gamma + d\Delta \tag{12}$$

where J is the resistance to fracture or fracture toughness of the soft tissue, dA represents the newly created crack surface area, $d\Gamma$ and $d\Delta$ denote the changes in the inelastic storage energy and elastic strain energy of soft tissue in time dt, respectively. Therefore, the high-speed waterjet impact gelatin model based on energy conservation is expressed as:

$$\pi \rho_w R^2 \left(\frac{1}{2} v_n^3 dt + g v_n^2 d^2 t \right) = JdA + d\Gamma + d\Delta \tag{13}$$

TABLE 1. Variable ranges.

Factor	Value		
Gelatin concentration	8wt. %	10wt. %	12wt. %
Water-jet speed/ mm.s^{-1}	1	2	3
Impact distance/ mm	5	7	9
Impact pressure/ MPa	2.2	2.9	3.6

It can be seen that the fluid dynamics and shape of the waterjet as well as the object material properties affect the entire impact process. Identifying the main influencing factors and analysing their relationship with separation and destruction effects will provide a basis for further optimising the dynamic parameters of the waterjet and corresponding application methods.

There is a strong non-linear coupling relationship between the above parameters. It is difficult to clarify the influence of one variable on another under reasonable assumptions. On the other hand, the viscoelastic and anisotropic characteristics of soft tissue also make the model assumptions overly idealised, resulting in large deviations in static results under theoretical analysis. Therefore, the current research on medical waterjet relies only on experimental methods to analyse the correlation between some influencing factors, while the target of these studies is a single gelatin sample, which often does not reflect the difference between it and the actual soft tissue under high-speed waterjet impact. To complete this research, the following experiment compares intra-gelatin variations and inter-specimen differences between gelatin and soft tissue.

III. MATERIALS AND METHODS

To analyse the destruction behaviour difference between gelatin and porcine liver under high-speed waterjet, gelatin concentration, impact distance, waterjet speed, and waterjet impact pressure are taken as variables of this study. Based on the principle of changing only a single variable, combined with the scope of operation space in clinical application, the range of each factor can be determined (Table 1). The range of gelatin concentration and impact pressure is taken from previously reported studies [10], [11], [14], considering that the fracture toughness of porcine liver in all biological soft tissues is relatively small, this study will set the gelatin concentration range from 8 wt.% to 12 wt.%. The waterjet impact distance and speed were determined according to the scope of clinical practice.

A. EQUIPMENT

Figure 2 shows a waterjet pump in which the linear motor drives the double-acting cylinders. The primary drive of the linear motor can reciprocate on the secondary, which provides tracks for the primary and its connecting parts. The linear motor is a DICI ZKK1-L514-FS2204 model, the driver is a Servotronix CDHD-0062AAP1, and the grating ruler (model RSF MS15.X4MK) feeds back displacement signals to the driver to realise a closed-loop, with a closed-loop resolution of 0.1 μm, an error of 0.5%, and a repeatability of $\pm$ 1 μm.

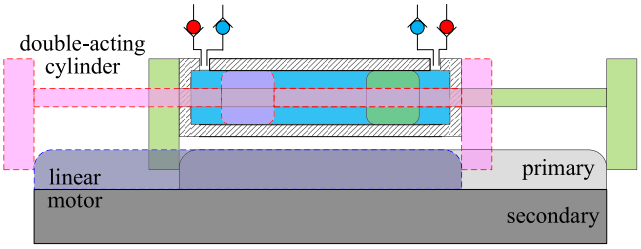

FIGURE 2. Waterjet pump: The solid and dashed lines are the two extreme positions of the piston, the piston reverses with the primary of the linear motor so that the left and right chambers of the plunger alternately absorb and drain water.

The plungers are fixed, and the piston reciprocates by the primary drive of the linear motor discharging or absorbing the liquid in the left and right chambers, thereby forming a continuous waterjet. The solid and dashed lines in Figure 2 are the two extreme positions of the piston and the primary drive of the linear motor. Such a structure can ensure the continuous absorption and discharge of the waterjet pump.

The waterjet pump and the nozzle are connected through a pipeline, and the outlet diameter of the nozzle is 0.2 mm. The linear motor drive velocity of the waterjet pump is controlled by a closed loop. The different speeds of the pistons cause differences in the outlet pressure of the waterjet pump. The relationship between the outlet pressure and linear motor driving velocity is shown in Figure 3, a non-linear positive correlation between the two was measured.

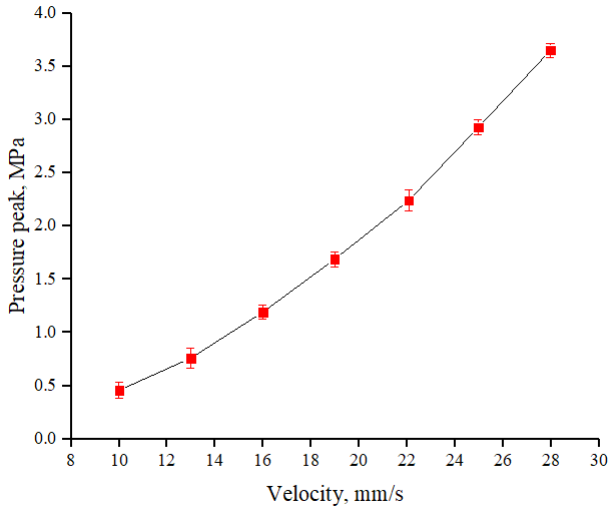

FIGURE 3. The relationship between the outlet pressure and linear motor drive velocity.

To achieve the single adjustment of the above indicators, a test bench was designed and installed as shown in Figure 4. The stage is driven by a screw-nut, and moves at a constant speed with a sample, and the moving distance and speed are adjusted by the stepping motor controller. The scale is marked on the slipways, so the impact distance and the impact start position are adjusted by the fixing bolt and

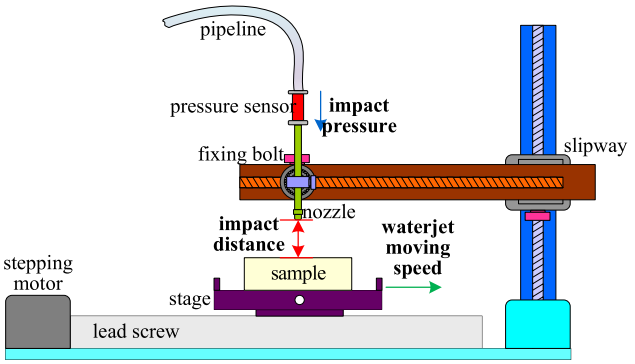

FIGURE 4. Test bench: the space position of the waterjet incidence can be adjusted by the scale of the slipway and the fixed bolt, and the relative speed was established by the movement of the stage.

slipway, respectively. The pressure sensor is installed between the nozzle and the pipeline. In this study, the pressure measured by the pressure sensor is defined as the impact pressure, the distance between the nozzle outlet and the upper surface of the specimen is defined as the impact distance, and the speed of the stage is defined as the speed of waterjet motion.

B. SAMPLE PREPARATION

The concentration of gelatin samples in this study ranged from 8 wt. % to 12 wt. % in 2 wt. % increments. The pig skin-extract Sigama48722 gelatin powder was dissolved in distilled water and stirred at a constant temperature (50 °C) for 1 hour. After the bubbles disappeared, it was poured into a mould and solidified at a constant temperature of 6 °C for 24 hours. Thus, a block-shaped sample with a length of 60 mm, width of 60 mm, and thickness of 20 mm was formed for testing. Three porcine livers from three female, 6-month-old pigs were obtained from a slaughterhouse within two hours post mortem; samples of the same size as the gelatin samples were prepared. This procedure was performed by Xuzhou Medical University staff authorised by the Science & Technology Department of Jiangsu, China, using authorised methods and in accordance with University Ethics Committee approval. Careful attention was paid to the orientation of the tissue samples. The samples were extracted perpendicular to the top surface of the livers and tested by the waterjet in that direction. The liver outer layer of membrane (capsule) was removed. Samples with large blood vessels or obvious pores were discarded in the experiments, so that only the properties of the tissue in the regions that were largely homogeneous were tested. Since the required sample thickness is larger than the thickness of certain sections of the liver, the sampling positions on the porcine liver are relatively concentrated.

C. MEASUREMENT METHODS

The nozzle is first fixed vertically on the junction plate of the transverse slipway and the sample is centred on the stage.

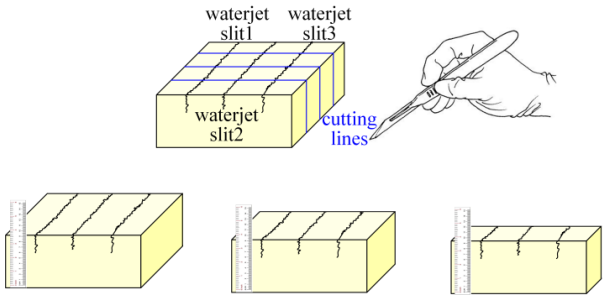

FIGURE 5. Impact depth measurement method: the vertical damage depth was measured at nine points on each sample.

The relative positions of the two slipways are then adjusted by the rotary gears such that the nozzle outlets are directly above the point of initial impact on the sample and meet the impact distance requirements. During the test, the stepping motors of the test bench and the waterjet pump are started at the same time, and then the sample moves with the stage. In terms of relative motion, the waterjet impact samples from one side to another. To minimise the deviation of the results caused by the difference in the sampling site of the porcine liver sample, the same parameter was measured three times on the same sample. After each impact test, the length of the fracture was measured. As shown in Figure 5, after the sample was cut three times at equal intervals on the test bench, three slits were formed on the surface, then the sample was cut, perpendicular to the crack direction along three equidistant cutting lines, using a scalpel, and the impact damage vertical depths at these three sections were measured using a dividing rule. In this way, each vertical damage depth data of a sample was averaged from nine data points.

D. STATISTICAL ANALYSIS METHODS

For tests between gelatin samples of different concentrations and porcine liver samples, the one-sample Kolmogorov-Smirnov test and Levene's test (absolute) were used to test for normality and equal variance, respectively. One way ANOVA analysis with the Tukey test was performed for all pairwise multiple comparisons with equal variance. Significance was determined by a p-value of 0.05 or less. If there are any groups with unequal variance, a Kruskal-Wallis H-test with a post-hoc Tukey-Kramer test with significance set at $p < 0.05$ was performed.

IV. RESULTS

Figure 6 illustrates the impact results of each sample at a 5 mm impact distance, comparing the damage depth of gelatin and porcine liver samples, and their relationship to various factors. Destruction depth of gelatin and porcine liver under high-speed waterjet impact is positively correlated with the impact pressure and negatively correlated with waterjet speed: the lower the gelatin concentration, the greater the damage depth under the same impact conditions. When the waterjet impact pressure is increased from 2.9 MPa to 3.6 MPa, the damage depth in porcine liver is significantly increased, while the damage depth in gelatin samples increases less.

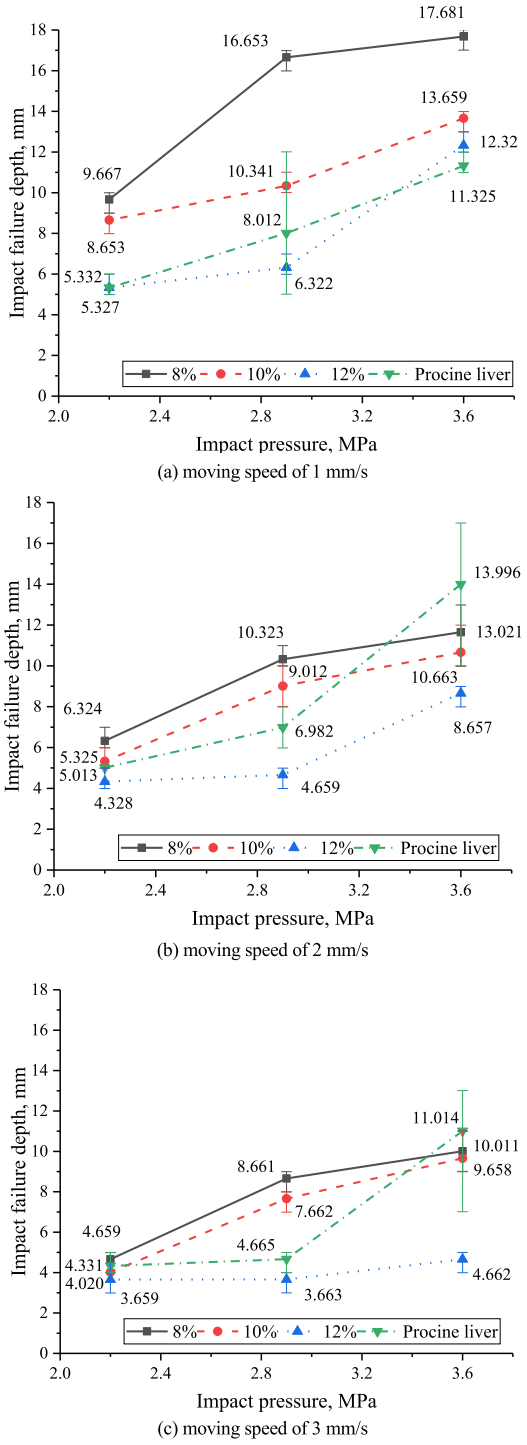

FIGURE 6. Impact depth at a 5 mm impact distance. (a), (b) and (c) respectively show the average damage depth (label value) of samples across porcine liver (green dotted line), 8 wt.% (black line), 10 wt.% (red dash line), and 12 wt.% (blue dot) as well as the up-down deviation at three different moving speeds.

Figure 7 shows the impact results of each sample at a 7 mm impact distance. The difference in damage depth between

gelatin and porcine liver samples at three waterjet speeds was described. The results show that the damage depth of gelatin and porcine liver increases with the increase of the impact pressure, and decreases with increasing speed. When the speed is increased from 1 mm/s to 2 mm/s, the reduction damage depth of the gelatin and porcine liver samples is greater than that from 2 mm/s to 3 mm/s. The average depth and ranges of the damage depth in porcine liver and the trend therein are closer to that in the 10 wt. % gelatin sample at the same impact distance.

Figure 8 demonstrates the impact results of each sample at an impact distance of 9 mm, and describes the relationship between the impact pressure and the impact damage depth of each sample at different waterjet speeds. At all three speeds, the depth of impact damage of porcine liver is greater than that at all concentrations of gelatin: at this impact distance, the average damage depth in porcine liver is closer to that in 8 wt. % gelatin samples, but the trend of impact damage depth in porcine liver with impact pressure is consistent with that of 10 wt. % gelatin samples, especially when the waterjet is moving at 2 mm/s or 3 mm/s.

V. DISCUSSION

In fact, the material mechanical response characteristics of soft tissue samples are often different due to location, age, and gender differences. These conclusions have been reported elsewhere [19], [20]: this means that under the same waterjet impact conditions, the damage depth distribution of porcine liver samples may be wider. In this study, the damage depths of samples under each impact condition were averaged from nine data points, and the upper and lower limits were marked, making the results statistically significant. At the same time, the trend and numerical distribution of damage depth between porcine liver samples and gelatin samples with different concentrations can statistically reflect the adaptability of gelatin to replace soft tissue under high-speed waterjet. In addition, the damage depths under different impact conditions were mutually verified, so that the comparison between each group of data points is also statistically significant. The statistical analysis results show that all the p values between the gelatin groups and the porcine liver groups are less than 0.05 when the impact distance is 5 mm or 7 mm, so there are no significant differences. The comparison of the data in Figures 6 to 8 indicates that due to the difference in fracture toughness, the impact depths of samples of different materials under high-speed waterjet impact are different. The higher the gelatin concentration, the greater the fracture toughness and the smaller the impact damage depth under the same impact conditions. Although the response trend of gelatin samples under waterjet impact is consistent with that of porcine liver samples, it can be seen that the mechanical response of gelatin is more similar to soft tissue obviating the need for it to be replaced by changing the configuration method of gelatin samples including the concentration thereon.

The separation efficiency trend of most of the porcine liver samples in the results shows that, within a certain range of impact pressures, the increase of pressure accelerates the separation of the sample. This suggests that adjusting the impact pressure can improve the separation efficiency of soft tissue. Each soft tissue corresponds to a sensitive pressure interval,

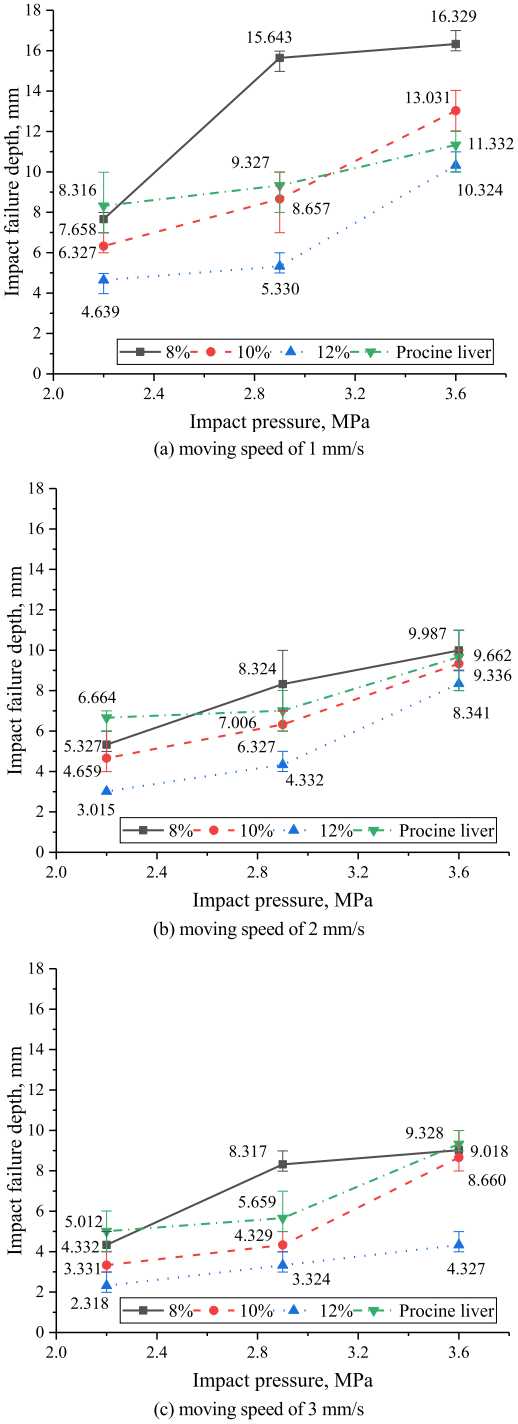

FIGURE 7. Impact depth at a 7 mm impact distance. (a), (b) and (c) respectively show the average damage depth (label value) of samples across porcine liver (green dotted line), 8 wt.% (black line), 10 wt.% (red dash line), and 12 wt.% (blue dot) as well as the up-down deviation at three different moving speeds.

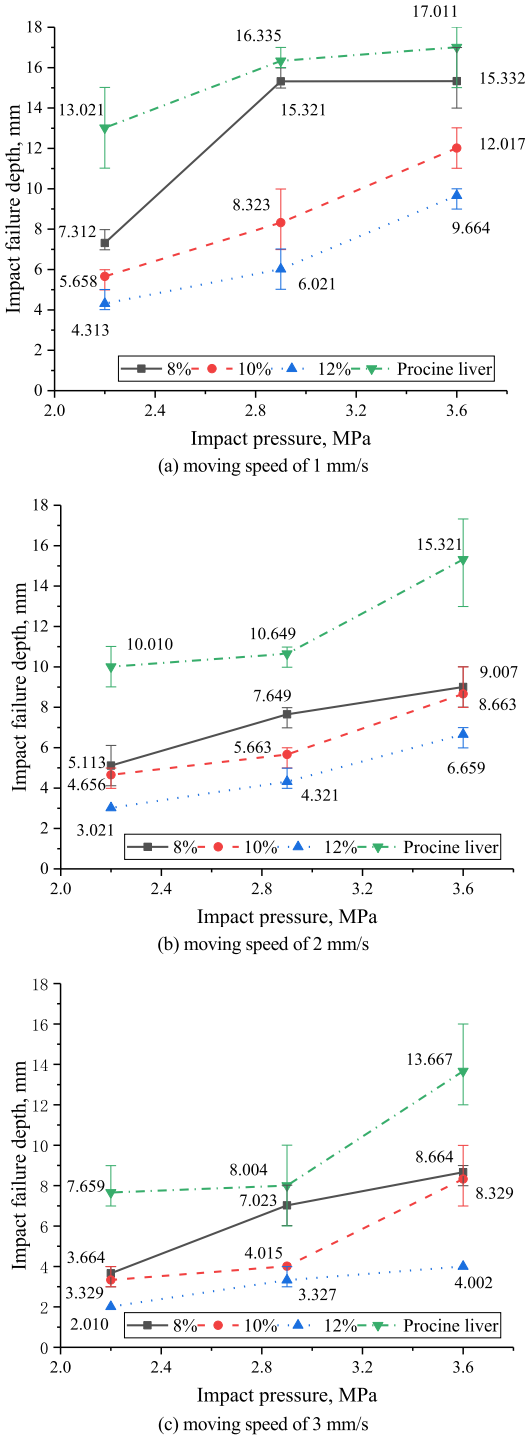

FIGURE 8. Impact depth at a 9 mm impact distance. (a), (b) and (c) respectively show the average damage depth (label value) of samples across porcine liver (green dotted line), 8 wt.% (black line), 10 wt.% (red dash line), and 12 wt.% (blue dot) as well as the up-down deviation at three different moving speeds.

and the separation and destruction efficiency in this interval is significantly accelerated with the increase of pressure, which is the key reason for the selective separation characteristics of medical waterjet separation technology.

The damage depth of the gelatin samples decreases with increasing impact distance under the same impact conditions. When the impact distance is 5 mm and the waterjet is moving at 1 mm/s, the average damage depth of gelatin is the largest; when the impact distance is 9 mm and the waterjet is moving at 3 mm/s, the average damage depth of gelatin is the smallest. For the porcine liver samples, the average impact damage depth is reduced when the impact distance is increased from 5 mm to 7 mm at each waterjet speed, and the average impact damage depth is increased when the impact distance is increased from 7 mm to 9 mm. The average damage depth of the gelatin samples at an impact distance of 5 mm is the greatest, while the average depth of damage in porcine liver samples is the largest at an impact distance of 9 mm. In the statistical test with the results of the porcine liver group, all groups had standard normal distributions, the variances were equal, and a one-way ANOVA with a post-hoc Tukey-Kramer test was performed with significance set at $p < 0.05$. While for the 12 wt. % gelatin samples, the statistical p values are all less than 0.05 at each waterjet moving speed ($p = 0.012$ of 1mm/s, $p = 0.021$ of 2mm/s, $p = 0.031$ of 3mm/s), for the 10 wt. % gelatin samples, the p is 0.038 under the impact condition that the waterjet moving speed is 1mm/s. There were statistically significant differences between the gelatin groups and the porcine liver groups under these conditions. The reason was shown in Figure 9, during the high-speed waterjet impact process, the liver tissue undergoes deformation opposite to the impact direction. This bulging deformation covers the impact distance at the initial state, and even causes the tissue surface to make contact with the nozzle outlet, which results in the observed waterjet fluid hydraulic dynamics changing. The larger deformation of the surface of the porcine liver sample, which results in a large gap between the actual impact distance and the designed impact distance. When the impact distance is adjusted to 9 mm, the deformation of the porcine liver samples cannot

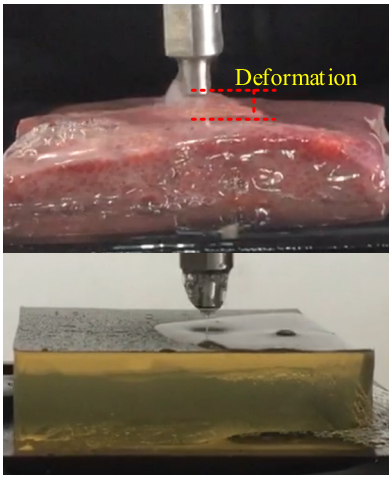

FIGURE 9. Differences in deformation between porcine liver and gelatin: the surface of porcine liver sample bulged, while the gelatin sample underwent almost no deformation.

completely cover this distance, and the waterjet flows in air before reaching the surface of the tissue samples.

Whether using gelatin samples or porcine liver samples, an increase in waterjet travel speed results in a decrease in the average damage depth; however, the proportional increase in speed does not lead to an inversely proportional reduction in the corresponding damage depth. For example, the average damage depth when moving at 2 mm/s is greater than half of the average damage depth at 1 mm/s; the average damage depth at 3 mm/s is greater than one third of the average damage depth at 1 mm/s. In particular, when the speed is increased from 2 mm/s to 3 mm/s, the average damage depth is remarkably less sensitive to changes in speed. This means that increasing the speed of movement improves the efficiency of material destruction. The specific clinical application requires a short operation time, low water consumption, and low risk of cross-infection, which is consistent with previously reported work [21]–[23].

The limitations of this study include the fact that the clamping force during clinical application was not simulated. Applying a clamping force will change the breaking force threshold of the sample and also affect the separation efficiency, however, reported research [24] shows that the influence of clamping force on the threshold of fracture force is clear, that is to say, the presence or absence of clamping force exerts no influence on the trend and conclusion reflected by this study. The influence of clamping force on separation efficiency will be analysed in future work. In addition, the trend of separation efficiency needs to be verified in soft tissue samples other than the liver.

VI. CONCLUSION

The destructive response behaviours of a certain concentration of gelatin samples and porcine liver tissue under some high-speed waterjet impact conditions are consistent. The difference under partial impact conditions is mainly attributed to the difference and anisotropy of gelatin material as a pure material. It is necessary to study gelatin-based composite biomimetic materials to compensate for the differences in mechanical properties of biological tissues.

Affected by the amount of deformation, the actual impact distance of soft tissue during the impact process is often much smaller than the initial impact distance. For porcine liver samples, the deformation characteristics determine that the actual impact distance can only be maintained when the impact distance is larger than 7mm. Gelatin bulges during high-speed waterjet impact, so the actual impact distance should be considered to compensate for this difference.

Gelatin samples and most porcine liver samples exhibit greater sensitivity to separation pressure over a specified pressure interval, indicating that different material properties correspond to different optimal pressure separation intervals. This will provide a reference for refining the control of medical waterjet hydraulic power and improving the clinical application of waterjet separation technology.

ACKNOWLEDGMENT

The authors thank the Editor and anonymous reviewers for their valuable comments and suggestions for improving the presentation of the manuscript.

REFERENCES

[1] S. Malekzadeh, M. J. Pfisterer, B. Wilson, H. Na, and M. K. Steehler, "A novel low-cost sinus surgery task trainer," *Otolaryngology Head Neck Surg.*, vol. 145, no. 4, pp. 530–533, 2011, doi: 10.1177/0194599811413373.

[2] C. E. Mendez-Probst, M. Vanjecek, H. Razvi, and P. A. Cadieux, "Ordnance gelatine as an *in vitro* tissue simulation scaffold for extracorporeal shock wave lithotripsy," *Urol. Res.*, vol. 38, no. 6, pp. 497–503, 2010, doi: 10.1007/s00240-010-0329-7.

[3] S. Liu, C. Xu, Y. Wen, G. Li, and J. Zhou, "Assessment of bullet effectiveness based on a human vulnerability model," *J. Roy. Army Med. Corps*, vol. 164, no. 3, pp. 172–178, 2018, doi: 10.1136/jramc-2017-000855.

[4] N. R. Park, K. H. Kim, J. S. Mo, and G. H. Yoon, "An experimental study on the effects of the head angle and bullet diameter on the penetration of a gelatin block," *Int. J. Impact Eng.*, vol. 106, pp. 73–85, Aug. 2017, doi: 10.1016/j.ijimpeng.2017.03.011.

[5] V. Sorgato, M. Berger, C. Emain, C. Vever-Bizet, J.-M. Dinten, G. Bourg-Heckly, and A. Planat-Chrétien, "Validation of optical properties quantification with a dual-step technique for biological tissue analysis," *J. Biomed. Opt.*, vol. 23, no. 9, 2018, Art. no. 0960029, doi: 10.1117/1.JBO.23.9.096002.

[6] C.-C. Shih, X. Qian, T. Ma, Z. Han, C.-C. Huang, Q. Zhou, and K. K. Shung, "Quantitative assessment of thin-layer tissue viscoelastic properties using ultrasonic micro-elastography with Lamb wave model," *IEEE Trans. Med. Imag.*, vol. 37, no. 8, pp. 1887–1898, Aug. 2018, doi: 10.1109/TMI.2018.2820157.

[7] S. Gorgieva, T. Vuherer, and V. Kokol, "Autofluorescence-aided assessment of integration and μ-structuring in chitosan/gelatin bilayer membranes with rapidly mineralized interface in relevance to guided tissue regeneration," *Mater. Sci. Eng. C*, vol. 93, pp. 226–241, Dec. 2018, doi: 10.1016/j.msec.2018.07.077.

[8] S. Wang, S. Guan, W. Li, D. Ge, J. Xu, C. Sun, T. Liu, and X. Ma, "3D culture of neural stem cells within conductive PEDOT layer-assembled chitosan/gelatin scaffolds for neural tissue engineering," *Mat. Sci. Eng. C*, vol. 93, pp. 890–901, Dec. 2018, doi: 10.1016/j.msec.2018.08.054.

[9] J. Breeze, N. Hunt, I. Gibb, G. James, A. Hepper, and J. Clasper, "Experimental penetration of fragment simulating projectiles into porcine tissues compared with simulants," *J. Forensic Legal Med.*, vol. 20, no. 4, pp. 296–299, 2013, doi: 10.1016/j.jflm.2012.12.007.

[10] T. Bahls, F. A. Fröhlich, A. Hellings, B. Deutschmann, and A. O. Albu-Schäffer, "Extending the capability of using a waterjet in surgical interventions by the use of robotics," *IEEE Trans. Biomed. Eng.*, vol. 64, no. 2, pp. 284–294, Feb. 2017, doi: 10.1109/TBME.2016.2553720.

[11] T. Seto, H. Yamamoto, K. Takayama, A. Nakagawa, and T. Tominaga, "Characteristics of an actuator-driven pulsed water jet generator to dissecting soft tissue," *Rev. Sci. Instrum.*, vol. 82, no. 5, 2011, Art. no. 055105, doi: 10.1063/1.3587069.

[12] F. Huang, Y. Lu, X. Liu, X. Ao, and L. Li, "Breakage mechanism of transverse isotropic rock subjected to high-pressure water jet," *Chin. J. Rock Mech. Eng.*, vol. 33, no. 7, pp. 1329–1335, 2014, doi: 10.13722/j.cnki.jrme.2014.07.004.

[13] C.-Y. Hsu, C.-C. Liang, T.-L. Teng, and A.-T. Nguyen, "A numerical study on high-speed water jet impact," *Ocean Eng.*, vol. 72, pp. 98–106, Nov. 2013, doi: 10.1016/j.oceaneng.2013.06.012.

[14] Y. Tatekura, M. Watanabe, K. Kobayashi, and T. Sanada, "Pressure generated at the instant of impact between a liquid droplet and solid surface," *Roy. Soc. Open Sci.*, vol. 5, no. 12, 2018, Art. no. 181101, doi: 10.1098/rsos.181101.

[15] A. Kiyama, Y. Tagawa, K. Ando, and M. Kameda, "Effects of a water hammer and cavitation on jet formation in a test tube," *J. Fluid Mech.*, vol. 787, pp. 224–236, Jan. 2016, doi: 10.1017/jfm.2015.690.

[16] D. Gao, Y. Lei, and B. Yao, "Dynamic soft tissue deformation estimation based on energy analysis," *Chin. J. Mech. Eng.*, vol. 29, no. 6, pp. 1167–1175, 2016, doi: 10.3901/CJME.2016.0909.111.

[17] Z. Hu, B. Zhang, and W. Sun, "Cutting characteristics of biological soft tissues," *CIRP Ann.*, vol. 61, no. 1, pp. 135–138, 2012, doi: 10.1016/j.cirp.2012.03.079.
[18] S. Liu, C. Xu, Y. Wen, S. Wang, J. Zhou, and X. Zhou, "Cavity dynamics in 10 wt% gelatin penetration of rifle bullet," *Int. J. Impact Eng.*, vol. 122, pp. 296–304, Dec. 2018, doi: 10.1016/j.ijimpeng.2018.09.006.
[19] D. B. MacManus, M. Maillet, S. O'Gorman, B. Pierrat, J. G. Murphy, and M. D. Gilchrist, "Sex- and age-specific mechanical properties of liver tissue under dynamic loading conditions," *J. Mech. Behav. Biomed. Mater.*, vol. 99, pp. 240–246, Nov. 2019, doi: 10.1016/j.jmbbm.2019.07.028.
[20] E. Etchell, L. Jugé, A. Hatt, R. Sinkus, and L. E. Bilston, "Liver stiffness values are lower in pediatric subjects than in adults and increase with age: A multifrequency MR elastography study," *Radiology*, vol. 283, no. 1, pp. 222–230, 2017, doi: 10.1148/radiol.2016160252.
[21] C. Nakanishi, T. Nakano, A. Nakagawa, C. Sato, M. Yamada, N. Kawagishi, T. Tominaga, and N. Ohuchi, "Evaluation of a newly developed piezo actuator-driven pulsed water jet system for liver resection in a surviving swine animal model," *Biomed. Eng. Online*, vol. 15, no. 1, p. 9, 2016, doi: 10.1186/s12938-016-0126-9.
[22] H. Kunikata, Y. Tanaka, N. Aizawa, A. Nakagawa, T. Tominaga, and T. Nakazawa, "Experimental application of piezoelectric actuator-driven pulsed water jets in retinal vascular surgery," *Transl. Vis. Sci. Technol.*, vol. 3, no. 6, p. 10, 2014, doi: 10.1167/tvst.3.6.10.
[23] T. Endo, Y. Takahashi, A. Nakagawa, K. Niizuma, M. Fujimura, and T. Tominaga, "Use of actuator-driven pulsed water jet in brain and spinal cord cavernous malformations resection," *Neurosurgery*, vol. 11, no. 3, pp. 394–403, 2015, doi: 10.1227/NEU.0000000000000867.
[24] Z. Hu, W. Sun, and B. Zhang, "Characterization of aortic tissue cutting process: Experimental investigation using porcine ascending aorta," *J. Mech. Behav. Biomed. Mater.*, vol. 18, pp. 81–89, Feb. 2013, doi: 10.1016/j.jmbbm.2012.10.017.

CHAO CAO was born in Jingdezhen, Jiangxi, China, in 1993. He received the B.S. degree in mechanical engineering from the China University of Mining and Technology, in 2010, where he is currently pursuing the Ph.D. degree with the School of Mechanical Engineering. His current research interests include hydromechanics, fluid machinery, and medical waterjet.

JIYUN ZHAO was born in Lianyungang, Jiangsu, China, in 1966. He received the B.S. degree in mining machinery and the M.S. degree in hydraulic transmission and control from the China University of Mining and Technology, in 1988 and 1992, respectively, and the Ph.D. degree in mechatronic engineering from Shanghai Jiao Tong University, in 1999. From 2003 to 2004, he was a Visiting Scholar with the Mechanical and Electrical Engineering Laboratory, University of Toronto, Canada. He is currently a Faculty Member with the School of Mechanical Engineering, China University of Mining and Technology. His research interests include hydraulic transmission and control, high-based hydraulic component, and intelligent equipment for dangerous environment.

GUILIN LI was born in Lianyungang, Jiangsu, China, in 1965. He received the B.S. degree in clinical medicine from Xuzhou Medical University, in 1989. He is currently the Director of the Xuzhou Maternal and Child Health Care Hospital. His research interests include surgical instruments and gynecological endoscope.

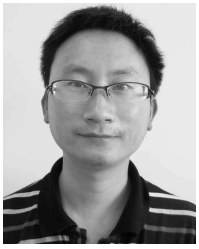

HAIGANG DING was born in Huaibei, Anhui, China, in 1981. He received the B.S. degree in mechanical engineering from Chang'an University, China, in 2004, and the M.S. degree in mechanical design and theory and the Ph.D. degree in mechatronic engineering from the China University of Mining and Technology, China, in 2009 and 2014, respectively. He is currently a Faculty Member with the School of Mechanical Engineering, China University of Mining and Technology. His research interest includes hydraulic transmission and control.

XIN JIN was born in Suzhou, Anhui, China, in 1983. She received the B.S. degree in clinical medicine from the Bengbu Medical College, in 2005. She is currently a Faculty Member with the Xuzhou Maternal and Child Health Care Hospital. Her research interests include surgical instruments and gynecological endoscope.

LIANGCHEN SONG was born in Suzhou, Anhui, China, in 1996. He received the B.S. degree in materials science and engineering from the China University of Mining and Technology, in 2018, where he is currently pursuing the master's degree with the School of Mechanical Engineering. His current research interests include mechanics of materials and fluid machinery.